Electronic Supporting Information for

Formation, Structure, and EPR Detection of a High Spin Fe^{IV}–Oxo Species Derived from Either an Fe^{III}–Oxo or Fe^{III}–OH Complex

David C. Lacy,[†] Rupal Gupta,[‡] Kari L. Stone,[†] John Greaves,[†] Joseph W. Ziller,[†] Michael P. Hendrich,*[‡] A. S. Borovik*[†]

[†]*Department of Chemistry, University of California-Irvine, 1102 Natural Sciences II, Irvine, California 92697-2025,* [‡]*Department of Chemistry, Carnegie Mellon University, Pittsburgh, Pennsylvania 15213, and the Department of Chemistry, Benedictine University, Lisle, Illinois 60532*

E-mail: aborovik@uci.edu, hendrich@andrew.cmu.edu

Contents

General Methods
All synthetic methods, unless otherwise stated, were performed under an argon atmosphere using a Vac-atmosphere dry box. All chemicals were purchased from commercial sources and used as received unless otherwise noted. Potassium hydride, dispersed in mineral oil, was filtered and washed with pentane (5 x 10 mL) and Et_2O (5 x 10 mL), dried on a vacuum line, and stored under an argon atmosphere. Synthesis of $K_2[Fe^{III}H_3buea(O)]$ was prepared following published procedures.[1] Ferrocenium tetrafluorborate ($[Fc]BF_4$) was prepared following literature methods.[2]

Synthesis

$K[Fe^{III}H_3buea(OH)]$. A modification of the published procedure was used.[1] The compound H_6buea (100. mg, 0.23 mmol) was deprotonated in 5 mL of DMA with KH (37 mg, 0.92 mmol) and allowed to stir till gas evolution ceased (~1 h). The resulting heterogeneous mixture was treated with $Fe(OAc)_2$ (40 mg, 0.23 mmol) and stirred for 1 h. Water (either ^{16}O or ^{18}O-labeled) (5 µL, 0.28 mmol) was added to the reaction and stirred for another 30 min. The yellow reaction was treated with I_2 (30 mg, 0.12 mmol) causing a color change from pale yellow to deep orange. The reaction was filtered and the orange filtrate was reduced to dryness. The orange residue was washed with Et_2O and then re-dissolved in a minimal amount of MeCN and filtered to remove insoluble material. Diffusion of Et_2O into the filtrate resulted in the formation of dark red crystals (67 mg, 41%) whose spectroscopic features matched those published previously.[1]

Isolation of solid $[Fe^{IV}H_3buea(O)]^-$ from $[Fe^{III}H_3buea(OH)]^-$. $K[Fe^{III}H_3buea(OH)]$ (52 mg, 0.094 mmol) was dissolved in 3 mL of MeCN and allowed to stir until the reaction mixture became homogeneous. The orange solution was treated with $[Fc]BF_4$ (28 mg, 0.10 mmol) causing a color change from orange to brown and the formation of brown precipitate that was immediately collected on a fine frit and washed with 1 mL of MeCN, 5 mL of Et_2O, and dried on the frit to afford 18 mg (35 %) of the product. FTIR (Nujol, cm^{-1}) ν(NH) 3275, 3213, ν (CO) 1596, 1543, ν ($Fe^{16}O$) 798, ν($Fe^{18}O$) 768; HR-ESI-MS $[Fe^{IV}H_3buea(^{16}O)]^-$: Exact mass calc'd for $C_{21}H_{42}N_7O_3Fe^{16}O$, 512.2648. Found 512.2634. $[Fe^{IV}H_3buea(^{18}O)]^-$: Exact mass calc'd for $C_{21}H_{42}N_7O_3Fe^{18}O$, 514.2691. Found 514.2676. λ_{max} (DMF, nm (ε, $M^{-1}cm^{-1}$)): 349 (4200), 440 (3100), 550 (1900), 808 (280). The visible absorbance spectra of $[FeCp_2]$ and $[FeCp_2]BF_4$ in DMF are shown in Figure S7. Only $[FeCp_2]^+$ contributed to the spectra shown in Figure 1, with a small peak at ~600 nm in the initial spectrum (red). The molar absorptivity was obtained by titration of $[Fe^{III}H_3buea(OH)]^-$ with $[FeCp_2]^+$ in DMF at -60˚C. The half life of the Fe(IV)O complex was determined by dissolving $[Fe^{IV}H_3buea(O)]^-$ (10 mg, 0.02 mmol) with DMF in a 25 mL volumetric flask. Spectrophotometeric analysis of data collected within a 1 cm cuvette at 25 ˚C allowed gave a pseudo first order rate constant.

Reaction with $[Fe^{IV}H_3buea(O)]^-$ with Diphenylhydrazine (DPH). Solid $[Fe^{IV}H_3buea(O)]^-$ (10 mg, 0.02 mmol) was dissolved in 1 mL of DMSO. The burgundy solution was treated with DPH (9 mg, 0.05 mmol) at room temperature, which caused an immediate color change from burgundy to orange. This reaction solution was allowed to stir for 24 h during which the DMSO was removed in vacuo. The solid was dissolved in 10 mL Et_2O and insoluble material was removed by filtration. The resulting filtrate (10 mL) was analyzed by GCMS and was obtained in greater than 90% yield.

Physical Methods
FTIR spectra were collected using a Varian 800 FTIR Scimitar Series spectrometer. Solution IR were collected using a Beckman solution IR cell. Absorption spectra were collected using a Cary 50 Scan UV-visible or a 8453 Agilent UV-Vis spectrometer equipped with an Unisoku Unispeks cryostat. Negative mode electrospray ionization electrospray mass spectra were collected using a Micromass MS Technologies LCT Premier Mass Spectrometer. The mass spectrum of $[Fe^{IV}H_3buea(^{16}O)]^-$ and $[Fe^{IV}H_3buea(^{18}O)]^-$ were collected at potentials of 400V and 750V,

respectively and calibrated with CsI and RbI. Cyclic voltammetric experiments were conducted using a CHI600C electrochemical analyzer following methods described previously.[3] A 2.0 mm glassy carbon electrode was used as the working electrode at scan velocities between 0.010 and 1.0 Vs^{-1}. A ferrocenium /ferrocene couple ([$Fc^{III/II}$]) was used to monitor the reference electrode (Ag^+/Ag).

Sample Preparation for Solution FTIR Measurements. K_2[Fe(III)H_3buea(O)] (25 mg, 0.033 mmol) was dissolved in 2mL of DMSO or DMF. The yellow orange reaction mixture was treated with [Fc]BF_4 (12 mg, 0.044 mmol) as a single addition causing the immediate color change from orange yellow to deep burgundy. Aliquots of this reaction were then subsequently transferred to a solution IR cell equipped with NaBr windows. The same spectrum (800-700 cm^{-1} region) was obtained for both solution.

EPR and Mössbauer Measurements

Sample preparation. Unless otherwise stated, all preparations were carried out at -60 °C in a cold-well within a drybox under an argon atmosphere.

[$Fe^{IV}H_3$buea(O)]$^-$ from [$Fe^{III}H_3$buea(O)]$^{2-}$. Ferrocenium tetrafluorborate ([Fc]BF_4) (30mg, 0.11 mmol) was dissolved in 2mL of DMF and thoroughly mixed. This deep blue homogeneous solution was added in one portion to another vial containing solid K_2[Fe(III)H_3buea(O)] (58 mg, 0.076 mmol) cooled to -60 °C. The new deep burgundy reaction mixture was filtered to remove undissolved Fe^{III}-O (~30 mg) and the filtrate was transferred to pre-cooled EPR tubes and Mössbauer cups (-60˚C) and stored in liquid nitrogen.

[$Fe^{IV}H_3$buea(O)]$^-$ from [$Fe^{III}H_3$buea(OH)]$^-$. The same procedure was followed as used for K_2[Fe(III)H_3buea(O)] with the following exceptions: solid [Fc]BF_4 (9 mg 0.033 mmol) was added to pre-cooled K[$Fe^{III}H_3$buea(OH)] (14 mg, 0.019 mmol) in 1 mL of DMF.

Data Collection and Analysis. X-band (9.28 GHz) EPR spectra were recorded on a Bruker 300 spectrometer equipped with an Oxford ESR-910 liquid helium cryostat and a dual mode microwave cavity. The quantification of signals is relative to a CuEDTA spin standard. The microwave frequency was calibrated with a frequency counter and the magnetic field with a NMR gaussmeter. The sample temperature of the cryostat was calibrated with a carbon-glass resistor (LakeShore CGR-1-1000) placed at the position of the sample in an EPR tube. The modulation frequency and amplitude was 100 kHz and 1.0 mT_{pp}. The EPR simulation software package SpinCounts was used to analyze the data.[4] The software diagonalizes the spin Hamiltonian $H = \beta_e \mathbf{B}\cdot\mathbf{g}\cdot\mathbf{S} + D\{\mathbf{S}_z^2 - S(S+1)/3 + E/D(\mathbf{S}_x^2 - \mathbf{S}_y^2)\}$, where the parameters have the usual definitions. The quantitative simulations are least-squares fits of the experimental spectra generated with consideration of all intensity factors, which allows computation of simulated spectra for a specified sample concentration. The Windows software package (SpinCount) is available for general application to any mono- or dinuclear metal complex by contacting M. Hendrich.

Mössbauer spectra were recorded with a Janis Research Super-Varitemp dewar. Isomer shifts are reported relative to Fe metal at 298 K. Least-square fitting of the spectra was performed with the WMOSS software package (WEB Research, Edina, MN). The Mössbauer parameters for ferrocence are in agreement with literature values.[5]

The states of the S = 2 spin manifold in zero magnetic field are approximately symmetric and antisymmetric combinations of the m_s magnetic states: $|1^{\pm}\rangle = (|+1\rangle \pm |-1\rangle)/\sqrt{2}$, $|2^{\pm}\rangle = (|+2\rangle \pm |-2\rangle)/\sqrt{2}$. The EPR signals are from transitions within the non-Kramers doublets $|1^{\pm}\rangle$ or $|2^{\pm}\rangle$. These transitions become allowed for $B_1 \,||\, B$ and $E/D > 0$.[6] The intensity of the signal is proportional to the square of the zero-field splitting of the respective doublet, Δ^2. The splitting Δ is proportional to $(E/D)^{ms}$, thus for the g~8 signal from the $|2^{\pm}\rangle$ doublet, the signal intensity is proportional to $(E/D)^4$.

Crystallography

A red crystal of approximate dimensions 0.27 x 0.29 x 0.36 mm was mounted on a glass fiber and transferred to a Bruker SMART APEX II diffractometer. The APEX2[1] program package was used to determine the unit-cell parameters and for data collection (25 sec/frame scan time for a sphere of diffraction data). The raw frame data was processed using SAINT[2] and SADABS[3] to yield the reflection data file. Subsequent calculations were carried out using the SHELXTL[4] program. The diffraction symmetry was 2/*m* and the systematic absences were consistent with the monoclinic space group $P2_1/n$ that was later determined to be correct. The salt crystallized with two DMF molecules. The structure was solved by direct methods and refined on F^2 by full-matrix least-squares techniques. The analytical scattering factors[5] for neutral atoms were used throughout the analysis. Hydrogen atoms were located from a difference-Fourier map and refined (x,y,z and U_{iso}). At convergence, wR2 = 0.0681 and Goof = 1.016 for 621 variables refined against 9198 data (0.74Å), R1 = 0.0250 for those 8281 data with I > 2.0σ(I).

Table S1. Electronic parameters of some relevant Fe^{IV} complexes.

Complex	*S*	*D* (cm^{-1})	*E/D*	*δ* (mm/s)	ΔE_Q (mm/s)	$g_{x,y}$, g_z	Reference
$[Fe^{IV}H_3buea(O)]^-$	2	4.0	0.03	0.02	0.43 [a]	n.d., 2.04	this work
$[Fe^{IV}(O)(TMG3tren)]^{2+}$	2	5.0	0.02	0.09	-0.29	n.d.	7
TauD	2	10.5	0.01	0.31	-0.88	n. d.	8
$[Fe^{IV}(O)(OH_2)_5]^{2+}$	2	9.7	0	0.38	-0.33	n. d.	9
$[Fe^{IV}(O)(TMC)(CH_3CN)]^{2+}$	1	26.95	0.07	0.17	1.23	2.10, 2.04	10, 11
$[Fe^{IV}(O)(N4Py)]^{2+}$	1	22.05	0	-0.04	0.93	2.03, 1.95	10, 11
$[Fe^{IV}NCl(\eta^4\text{-MAC*})]^-$	2	-2.6	0.14	-0.04	0.89	n.d., 1.8	12

[a]Sign is undetermined.

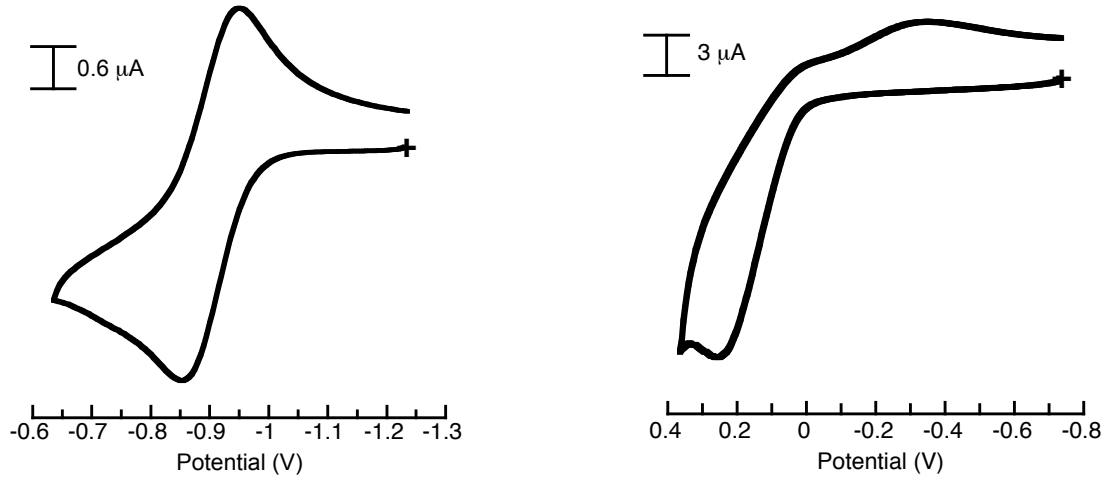

Figure S1. Cyclic voltammograms for the oxidation of $[Fe^{III}H_3buea(O)]^{2-}$ (left) and $[Fe^{III}H_3buea(OH)]^{-}$ (right) under the same cell conditions. Data were collected at a scan rate of 0.010 V/s.

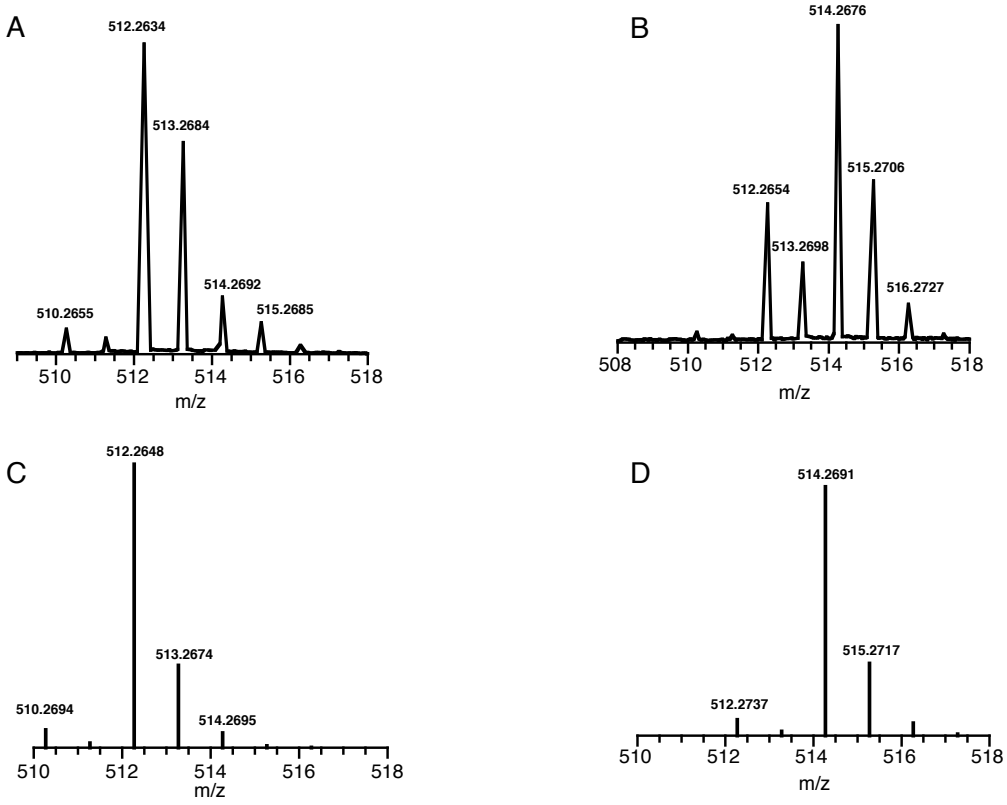

Figure S2. Negative-mode ESI mass spectra for $[Fe^{IV}H_3buea(^{16}O)]^{-}$ (**A**) and $[Fe^{IV}H_3buea(^{18}O)]^{-}$ (**B**) and their calculated spectra (**C**, **D**), respectively. The samples were prepared from $[Fe^{III}H_3buea(OH)]^{-}$. The M+1 peaks in the observed mass spectrum originates from the Fe(III)OH complex. This is experimentally confirmed from collecting mass spectra of the starting Fe(III)OH complex. Another observation that confirms the presence of the M+1 peak originating from Fe(III)OH complex is the ionization potential dependence of the spectrum. At high ionization potentials (1000-4000V) the spectrum contains mostly the M+1 peak. Lowering the ionization potential (as low as 400V and no higher than 700V) the M+1 peak decreases dramatically and the peak associated with the Fe(IV)O ion persists as the major species.

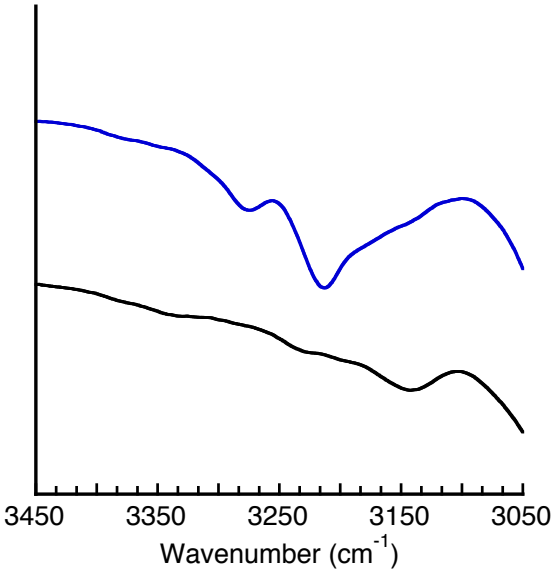

Figure S3. Solid-state FTIR spectra of $[Fe^{IV}H_3buea(O)]^-$ (–) and $[Fe^{III}H_3buea(O)]^{2-}$ (–) highlighting the peaks associated with the NH groups.

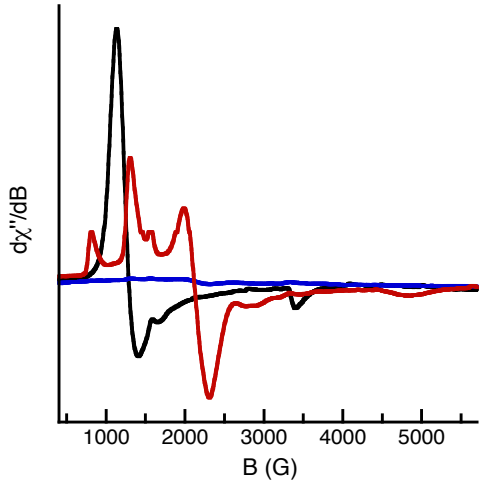

Figure S4. Perpendicular-mode X-band EPR spectra of $[Fe^{III}H_3buea(O)]^{2-}$ (black), the spectrum after treatment with $[FeCp_2]^+$ (blue), and after warming showing the conversion to $[Fe^{III}H_3buea(OH)]^-$ (red).

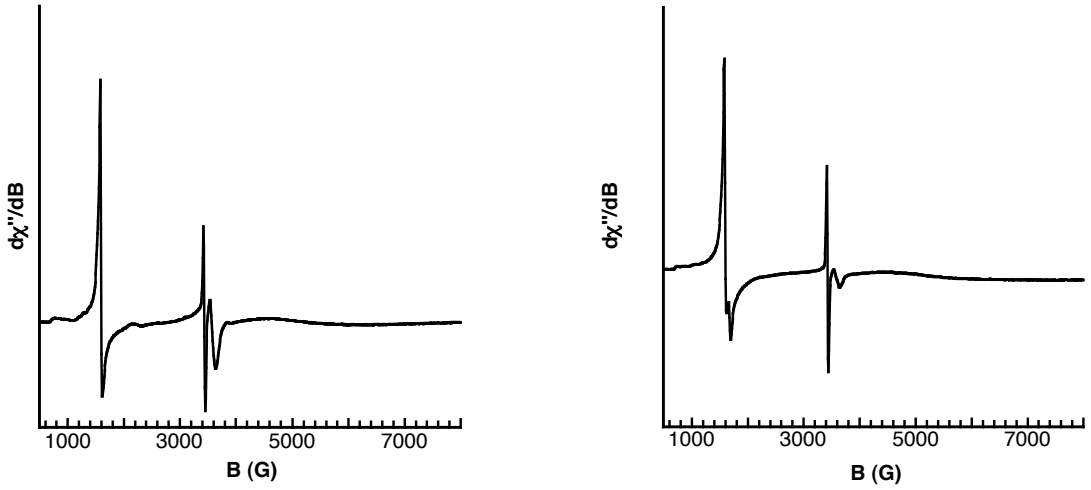

Figure S5. Perpendicular-mode X-band EPR spectra after oxidation of $[Fe^{III}H_3buea(O)]^{2-}$ (left) and $[Fe^{III}H_3buea(OH)]^{-}$ (right) with $[FeCp_2]^{+}$.

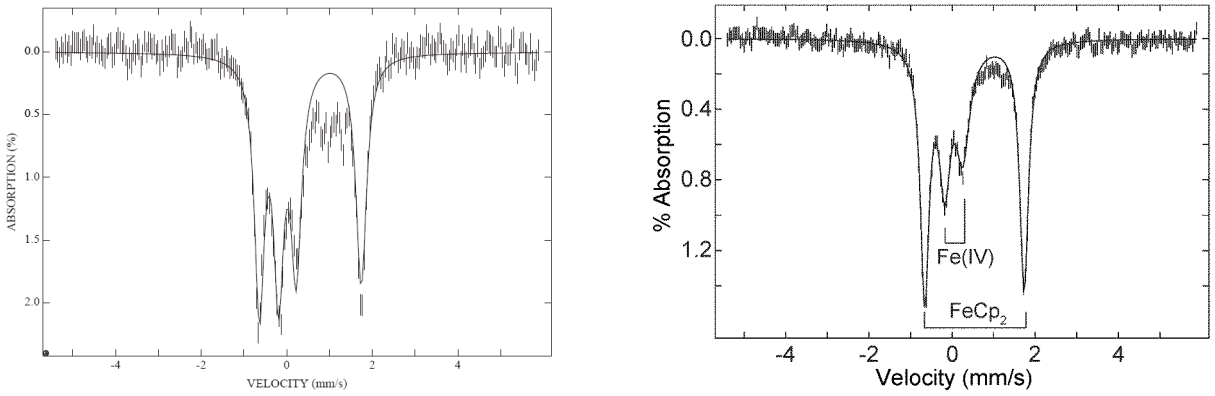

Figure S6. Mössbauer spectra (4.2 K) of $[Fe^{IV}H_3buea(O)]^{-}$ prepared from the oxidation of $[Fe^{III}H_3buea(OH)]^{-}$ with $[FeCp_2]^{+}$ in solution (left) and $[Fe^{III}H_3buea(O)]^{2-}$ with $[FeCp_2]^{+}$ (right), in absence of a magnetic field. The outer doublet in each spectrum is from $[FeCp_2]$, the other product from the reaction. The observed parameters for $[FeCp_2]$ are δ = 0.55 mm/s and ΔE_Q = 2.4 mm/s.

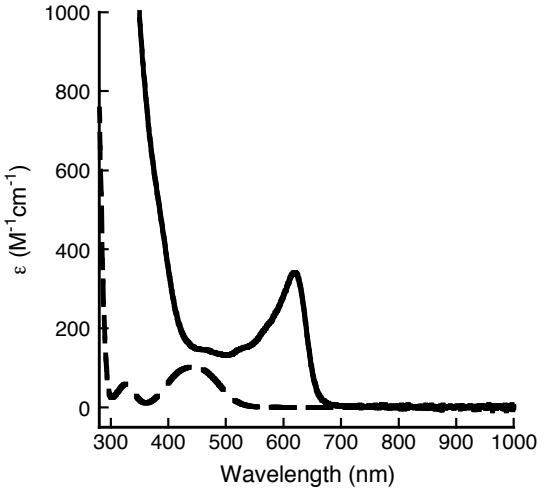

Figure S7. Absorbance spectra of $[Fe^{II}Cp_2]$ (— —) and $[Fe^{III}Cp_2]^+$ (—) measured in DMF.

References

1. MacBeth, C. E.; Gupta, R.; Mitchell-Koch, K. R.; Young, V. G., Jr.; Lushington, G. H.; Thompson, W. H.; Hendrich, M. P.; Borovik, A. S. *J. Am. Chem. Soc.* **2004**, *126*, 2556-2567.
2. Connelly, N. G.; Geiger, W. E. *Chem. Rev.* **1996**, *96*, 877-910.
3. Ray, M; Hammes, B. S.; Yap, G. P. A.; Rheingold, Liable-Sands, L.; Borovik, A. S. *Inorg. Chem.* **1998**, *37*, 1527-1533.
4. Golombek, A. P.; Hendrich, M. P., *J. Magn. Reson.* **2003**, *165*, 33–48.
5. Lesikar, A. V., *J. of Chem. Phys.* **1964**, *40*, 2746-7.
6. Hendrich and Debrunner, *Biophys. J.* **1989**.
7. England, J.; Martinho, M.; Farquhar, E. R.; Frisch, J. R.; Bominaar, E. L.; Münck, E.; Que, L., Jr. *Angew. Chem. Int. Ed.* **2009**, *48*, 3622-3626.
8. Price, J. C.; Barr, E. W.; Tirupati, B.; Bollinger, J. M., Jr.; Krebs, C. *Biochemistry* **2003,** *42,* 7497-7508.
9. Pestovsky, O.; Stoian, S.; Bominaar, E. L.; Shan, X.; Münck, E.; Que, L., Jr.; Bakac, A. *Angew. Chem., Int. Ed.* **2005**, *44*, 6871-6874.
10. Krzystek, J.; England, J.; Ray, K.; Ozarowski, A.; Smirnov, D.; Que, L., Jr.; Telser, J. *Inorg. Chem.* **2008**, *47*, 1727-1752.
11. Jensen, M. P.; Costas, M.; Raymond Y. N. Ho, R. Y. N.; Kaizer, J.; Payeras, A. M.; Münck, E.; Que, L., Jr.; Rohde, J.-W.; Stubna, A. *J. Am. Chem. Soc.* **2005**, *127*, 10512-10525.
12. K. L; Fox, B. F.; Hendrich, M. P.; Collins, T. J.; Rickard, C. E. F.; L. Wright, L. J.; Münck, E. *J. Am. Chem.* Soc. **1993**, *115*, 6746-6757.